Check for updates

Cytochrome respiration pathway and sulphur metabolism sustain stress tolerance to low temperature in the Antarctic species *Colobanthus quitensis*

María José Clemente-Moreno[1]*, Nooshin Omranian[2,3]*, Patricia Sáez[4], Carlos María Figueroa[5], Néstor Del-Saz[6], Mhartyn Elso[4], Leticia Poblete[4], Isabel Orf [7], Alvaro Cuadros-Inostroza[8], Lohengrin Cavieres[9] (iD), León Bravo[10,11], Alisdair Fernie[12] (iD), Miquel Ribas-Carbó[1], Jaume Flexas[1], Zoran Nikoloski[2,3,13], Yariv Brotman[7] and Jorge Gago[1] (iD)

[1]Research Group on Plant Biology under Mediterranean Conditions, Instituto de Agroecología y Economía del Agua (INAGEA), Universitat de les Illes Balears (UIB), cta. Valldemossa km 7, 5, 07122, Palma de Mallorca, Spain; [2]Systems Biology and Mathematical Modeling Group, Max-Planck-Institut für Molekulare Pflanzenphysiologie, 14476, Potsdam-Golm, Germany; [3]Bioinformatics, Institute of Biochemistry and Biology, University of Potsdam, Karl-Liebknecht-Str. 24–25, 14476, Potsdam, Germany; [4]Laboratorio Cultivo de Tejidos Vegetales, Centro de Biotecnología, Departamento de Silvicultura, Facultad de Ciencias Forestales, Universidad de Concepción, 4030000, Concepción, Chile; [5]Instituto de Agrobiotecnología del Litoral, UNL, CONICET, FBCB, 3000, Santa Fe, Argentina; [6]Laboratorio de Fisiología Vegetal, Departamento de Botánica, Facultad de Ciencias Naturales y Oceanográficas, Universidad de Concepción, 4030000, Concepción, Chile; [7]Department of Life Sciences, Ben Gurion University of the Negev, 8410501, Beer Sheva, Israel; [8]Metasysx GmbH, Am Mühlenberg 11, 14476, Potsdam, Germany; [9]ECOBIOSIS, Departamento de Botánica, Facultad de Ciencias Naturales y Oceanográficas, Universidad de Concepción, 4030000, Concepción, Chile; [10]Laboratorio de Fisiología y Biología Molecular Vegetal, Departamento de Cs. Agronómicas y Recursos Naturales, Facultad de Ciencias Agropecuarias y Forestales, Instituto de Agroindustria, Universidad de La Frontera, Temuco, Chile; [11]Center of Plant, Soil Interaction and Natural Resources Biotechnology, Scientific and Technological Bioresource Nucleus, Universidad de La Frontera, 4811230, Temuco, Chile; [12]Central Metabolism Group, Molecular Physiology Department, Max-Planck-Institut für Molekulare Pflanzenphysiologie, 14476, Golm, Germany; [13]Center of Plant System Biology and Biotechnology (CPSBB), 4000, Plovdiv, Bulgaria

Summary

• Understanding the strategies employed by plant species that live in extreme environments offers the possibility to discover stress tolerance mechanisms. We studied the physiological, antioxidant and metabolic responses to three temperature conditions (4, 15, and 23°C) of *Colobanthus quitensis* (CQ), one of the only two native vascular species in Antarctica. We also employed *Dianthus chinensis* (DC), to asses the effects of the treatments in a non-Antarctic species from the same family.

• Using fused LASSO modelling, we associated physiological and biochemical antioxidant responses with primary metabolism. This approach allowed us to highlight the metabolic pathways driving the response specific to CQ.

• Low temperature imposed dramatic reductions in photosynthesis (up to 88%) but not in respiration (sustaining rates of 3.0–4.2 μmol CO_2 m^{-2} s^{-1}) in CQ, and no change in the physiological stress parameters was found. Its notable antioxidant capacity and mitochondrial cytochrome respiratory activity (20 and two times higher than DC, respectively), which ensure ATP production even at low temperature, was significantly associated with sulphur-containing metabolites and polyamines.

• Our findings potentially open new biotechnological opportunities regarding the role of antioxidant compounds and respiratory mechanisms associated with sulphur metabolism in stress tolerance strategies to low temperature.

Introduction

Colobanthus quitensis (Kunth) Bartl. (CQ; Caryophyllaceae family) is one of the two vascular plants that were naturally able to colonize the scarce Antarctic ice-free areas (Kappen, 1999).

Antarctica is probably the most extreme continent for supporting life: it is the coldest, driest, and windiest continent on Earth. Climatic conditions are so hostile that, even during summer, plants frequently face subzero temperatures, strong winds, and very long photoperiods. Moreover, water availability is restricted to ice and glacier melting. In combination with strong dry winds (that impose elevated evaporation rates), this make life extremely

*These authors contributed equally to this work.

difficult (Bramley-Alves *et al.*, 2014). Likewise, CQ is also distributed along high elevations in the Andes up to Mexico, where it inhabits sites with similar cold and harsh conditions. This has awakened an increased interest to describe the physiological and molecular adaptations that allow CQ to cope with such an extreme environment – for a review, see Cavieres *et al.* (2016).

Under optimal conditions, CQ shows a photosynthetic range from 8 to 11 µmol CO_2 m^{-2} s^{-1}; interestingly, it can sustain positive net assimilation rates (*c.* 30% of their maximum) even at 0°C (Xiong *et al.*, 1999; Sáez *et al.*, 2017). High respiration rates (2–3 µmol CO_2 m^{-2} s^{-1}) have been described in CQ, which is ranked in the upper range for herbaceous plants in a comparative study of 899 species (Atkin *et al.*, 2015). It was suggested that, under low temperature, photosynthesis could be an important electron sink and thus would help alleviate oxidative stress (Xiong *et al.*, 1999), in combination with photoprotective mechanisms, such as nonphotochemical quenching and heat dissipation by the xanthophyll cycle, rather than by primary antioxidants (Pérez-Torres *et al.*, 2004a). However, in addition to ensuring high photosynthesis rates at low temperature, CQ also has to use other mechanisms to survive in the extreme environments like Antarctica or high altitudes (low temperature, drought, and an extremely variable radiation; Cavieres *et al.*, 2016).

Low temperatures enhance stress levels by impairing primary and secondary photosynthetic reactions and promoting the generation of reactive oxygen species (ROS). Thus, energy dissipation and regulation of the oxidative stress status should be a priority to maintain cell homeostasis (Hoermiller *et al.*, 2017). Under oxidative stress, mitochondrial respiration has been suggested to modulate the formation of ROS, by dissipating reductants from both mitochondria and chloroplast (Tezara *et al.*, 2008; Atkin & Macherel, 2009; Florez-Sarasa *et al.*, 2016); indeed, differential changes of the cytochrome oxidase pathway (COP) and alternative oxidase (AOX) pathway (AOP) could also modulate cell oxidative stress and energy levels (Del-Saz *et al.*, 2018). Low temperature is reputed for decreasing rates of respiration by inducing malfunction of components of the mitochondrial electron transport chain and TCA cycle (Atkin & Tjoelker, 2003) and increasing AOX activity (Ribas-Carbó *et al.*, 2000; Heidarvand *et al.*, 2017). By using *aox1a* Arabidopsis mutants with reduced levels of AOX protein, it was shown that AOX was involved in the balance of primary metabolism at low temperature (Watanabe *et al.*, 2008). Notwithstanding, AOX activity may decrease the energy efficiency of respiration (O'Leary *et al.*, 2019). Interestingly, Arctic plants have shown the ability to modulate the respiratory energy efficiency for the benefit of ATP synthesis via the COP (Kornfeld *et al.*, 2013). Thus, it might be expected that, in CQ, respiration via the COP could contribute to tolerate low temperatures, considering its high rates of respiration (Del-Saz *et al.*, 2018; O'Leary *et al.*, 2019).

The plant metabolome is extraordinarily dynamic and drives plant–environment responses (Brunetti *et al.*, 2013). Thus, metabolic information can be linked to the physiological responses to obtain further specific knowledge, which could help us to understand the mechanisms underlying these responses (Obata & Fernie, 2012; Sulpice *et al.*, 2013; Gago *et al.*, 2016,

2017; Flexas & Gago, 2018). In addition, statistical modelling in systems biology is used to identify molecular markers (e.g. genes, proteins, and metabolites) that are predictive of complex physiological traits in multiple environments and/or species. Such conserved associations between molecular markers and traits can, in turn, be complemented with approaches that are specific to a particular environment and/or species (Wen *et al.*, 2015; Li *et al.*, 2016; Omranian *et al.*, 2016; de Abreu e Lima *et al.*, 2018). The leaf metabolome has shed light on mitochondrial respiration regulation (Nunes-Nesi *et al.*, 2010; Araújo *et al.*, 2011, 2012; O'Leary *et al.*, 2019), particularly on the role of AOX activity in responses to environmental stresses (Del-Saz *et al.*, 2018). It has been shown that sugars (maltose, xylose), organic acids (malate, fumarate, citrate), and amino acids (asparagine, β-alanine) are correlated with *in vivo* AOX activity in different species under high irradiance, salinity, and phosphorus (P) deficiency as a mechanism associated with the consumption of reducing equivalents (Del-Saz *et al.*, 2016, 2018; Florez-Sarasa *et al.*, 2016; O'Leary *et al.*, 2019).

Considering the high mitochondrial respiration rates reported in CQ, we hypothesize that respiration might play a relevant role under low temperature stress, to alleviate the altered redox status and provide energy and carbon (C) skeletons to sustain cell homeostasis and antioxidant responses. To assess this hypothesis, we combined ecophysiology, biochemistry, metabolomics, and statistical modelling approaches to understand the mechanisms leading to stress tolerance in two CQ ecotypes (Antarctic and Andean) grown at three different temperatures (i.e. 4, 15, and 23°C). Moreover, China pink, *Dianthus chinensis* (DC), a non-Antarctic cultivated species from the same family as CQ (Caryophyllaeace) was also included in our experiment as a reference for our stress treatments. The resulting data were combined and analysed through the integrative statistical fused LASSO modelling to associate complex physiological traits with metabolic markers. Finally, to validate the main results from the statistical modelling, we performed further experiments focused on characterizing the *in vivo* respiration and total antioxidant capacity of CQ. Taken together, we integrated ecophysiological, biochemical, and molecular technologies to identify the mechanisms that allow CQ to withstand the most inhospitable continent on Earth.

Materials and Methods

Collection sites and climatic conditions

CQ (Caryophyllaceae, pearlwort) was collected from King George Island in the South Shetlands, near to the Henryk Arctowski Polish Antarctic Station (62°09′S, 58°28′W, December 2015) and from the central Chilean Andes at 2650 m elevation Cerro La Parva–Farallones (33°19′S, 70°17′W, December 2015; Fig. 1).

The mean air temperature during summer months in the Henryk Arctowski Station is *c.* 3°C, with maximum and minimum values of 12°C and −5°C, respectively (Fig. 1d). Most days are characterized by overcast conditions with short periods of high
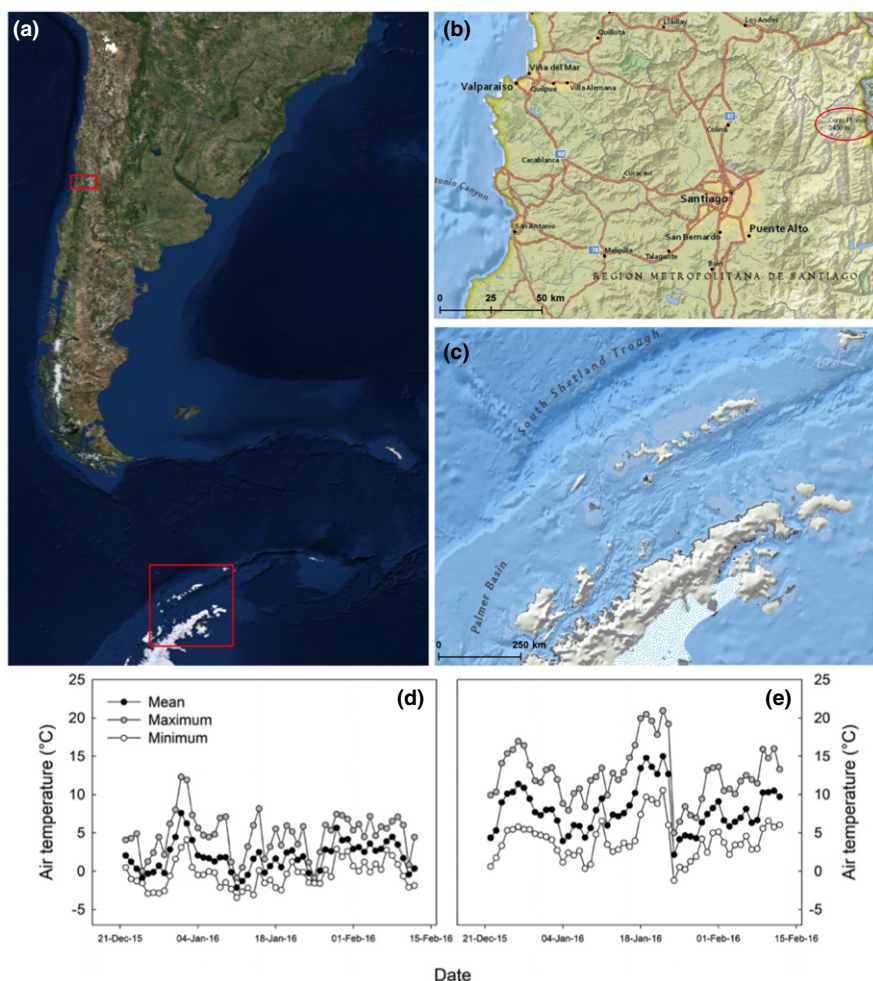
Fig. 1 Sampling sites and mean air temperatures during the growing season in Antarctica and Andean range. (a) Sampling sites in South America and Antarctica. (b) Zoomed image from (a) of Cerro La Parva in the Andean range (2650 m asl, 33°19′S; 70°17′W). (c) Zoomed image from (a) of King George Island (South Shetland, Maritime Antarctica, 62°09′S, 58°28′W) and Lagotellerie Island (Antarctic Peninsula, 67°53′20″S, 67°25′30″W). (d, e) Maximum, average, and minimum air temperatures for the period 21 December 2015–15 February 2016 (the middle of the growing season) in (d) King George Island (near H. Arctowski Research Station) and (e) Cerro La Parva (Andean range).

irradiance (*c.* 2000 µmol m^{-2} s^{-1}). The mean annual precipitation (which mostly falls as snow) is *c.* 700 mm (Angiel *et al.*, 2010). The central Chilean Andes climate is alpine, with strong influence of the Mediterranean-type climate that characterizes the lowlands (Arroyo *et al.*, 1999). The average air temperature during the growing season is 7–8.5°C, with maximum and minimum values of 21°C and −6°C, respectively (Casanova-Katny *et al.*, 2006; Cavieres *et al.*, 2007). In contrast to Antarctica, irradiance levels are constantly high on most days, with values of 2000 µmol m^{-2} s^{-1} for several hours (Casanova-Katny *et al.*, 2006). The mean annual precipitation is *c.* 431 mm, mainly falling as snow between April and October (for more climatic details, see Methods S1). For simplification, throughout the remainder of this paper CQ$_A$ and CQ$_F$ are used for CQ from Antarctica (King George Island) and from Farallones–La Parva in the Andes, respectively.

Growth conditions and experimental setup

We reproduced the two CQ ecotypes vegetatively in plastic pots, using a sterile soil–vermiculite–peat mixture (3 : 1 : 1 v/v) and maintained at 15°C (Xiong *et al.*, 1999; Sáez *et al.*, 2017), in a growth chamber with irradiance of 300 µmol m^{-2} s^{-1} and

16 h : 8 h photoperiod. Plants were watered to full soil capacity every 2–3 d and fertilized once a week. We also grew DC from the same Caryophyllaceae family as a reference species to validate the effect of the temperature treatments in a non-Antarctic species. DC is an ornamental species, originated from temperate grasslands/shrublands biomes typically characterized by cold winters and reduced precipitation in northeast Asia (Whittaker, 1975; Fu *et al.,* 2008). DC was maintained at the same conditions as CQ (except temperature at 23°C) until the beginning of the experiment. For the experiment, plants were randomly divided into subsets and placed in different growth chambers for the temperature treatments of 4, 15, and 23°C for 12 d. This range was chosen to correspond to the day average temperature of the Antarctic summer, the optimum photosynthetic temperature determined for this species, and the optimum photosynthetical temperature for temperate crops, respectively (Yamori *et al.*, 2014; Sáez *et al.*, 2018); more details are given in Methods S1.

Subsequently, to validate the results of the first set of experiments and modelling, we performed two additional experiments focusing on the 15 C and 4°C temperature treatments (in which were found the main stress differences), and we just used the Antarctic ecotype (CQ$_A$) in parallel with the reference non-Antarctic species, DC.

Gas-exchange measurements and photosynthesis models

We employed an infrared gas analyser (Li-6400-40, Li-Cor Inc., Lincoln, NE, USA) coupled with a Chl fluorimeter (Li-6400-40, 2 cm^2 chamber; Li-Cor) to measure gas-exchange and Chl fluorescence in fully expanded leaves. Measurement conditions were set up to block temperature (4, 15, or 23°C, same as the growth conditions), vapour pressure deficit at c. 1.5 kPa, CO_2 concentration was fixed at 400 µmol CO_2 per mole of air, and light at 1000 µmol m^{-2} s^{-1} photosynthetic photon flux density (90 : 10, red : blue light).

Once leaf gas-exchange steady-state conditions were observed, CO_2 photosynthetic response curves were performed using CO_2 chamber concentration C_a steps of 400, 300, 200, 100, and 75 ppm and back to 400 ppm CO_2. CO_2 leakage was corrected following the methodology described by Flexas et al. (2007).

Day respiration R_{day} was considered as half of the dark-adapted mitochondrial respiration R_{dark} after a minimum 30 min under dark conditions (Niinemets et al., 2005). Photorespiration P_R and the product of α (absorbance) and β (partition between PSII and PSI) to correct the electron transport rate (ETR) were estimated by combining fluorescence and gas-exchange measurements per each species and treatment. The product $\alpha \times \beta$ was estimated through low-oxygen (O_2) light curves (< 1% [O_2]); under these nonphotorespiratory conditions, P_R is greatly reduced, making it possible to compare the measured relationship between the ETR and the rate of photosynthetic electron transport with the theoretical relationship based on photosynthetic stoichiometry (Valentini et al., 1995) (Table S1). Thus, the ETR values were corrected by the previous product $\alpha * \beta$ and subsequently, the chloroplastic CO_2 concentration (C_c) and the mesophyll conductance (g_m) are calculated according to Harley et al. (1992). The $V_{c,max}$ was estimated following Farquhar et al. (1980) after converting net CO_2 assimilation rate (A_N)–internal [CO_2] into A_N–C_c curves using the estimated g_m. We used previously published Rubisco specificity factors $S_{c/o}$ and kinetic values at the different temperatures for each species (Sáez et al., 2017). For DC, we used CQ data, as it is the most similar species found in the literature. The chloroplast CO_2 compensation point Γ^* was calculated from the $S_{c/o}$ measured in vitro, as described by von Caemmerer (2000). Leaf mass area (LMA) was calculated as described previously (Tosens et al., 2016).

Antioxidant responses and oxidative stress parameters

Leaf samples were harvested (1 g FW) and immediately frozen in liquid nitrogen (N) for biochemical assays as lipid peroxidation, glutathione (GSH) quantification, and total antioxidant activity. For enzymatic assays, frozen samples were ground in a mortar and homogenized with 50 mM Tris-acetate (pH 6.0) extraction buffer containing: 0.1 mM EDTA, 2 mM cysteine, 2% (w/v) insoluble poly-vinylpolypyrrolidone, and 0.2% (v/v) Triton X-100. For ascorbate peroxidase (APX; EC 1.11.1.11), fresh leaves samples were used, and 20 mM sodium ascorbate was added to the extraction buffer. Samples were centrifuged for 20 min at 14 000 g and 4°C. APX, catalase (CAT; EC 1.11.1.6), and peroxidase (POX; EC 1.11.1.7) activities were measured as described in Díaz-Vivancos et al. (2006, 2008). Protein content was estimated according to Bradford (1976). Activity assays were performed using an Epoch spectrophotometer (Biotec Instruments, USA) at 25°C.

Lipid peroxidation was estimated by determining the concentration of thiobarbituric acid-reactive substances (TBARS; Cakmak & Horst, 1991). Total, reduced, and oxidized glutathione (GSHt, GSH, and GSSG, respectively) were assayed according to the method of Zhang & Kirkham (1996). Frozen leaf samples were homogenized in 10% metaphosphoric acid, and GSH determination was measured as described in Clemente-Moreno et al. (2013). Total antioxidant capacity of leaf samples was calculated by 2,2′-azino-bis(3-ethylbenzothiazoline-6-sulphonic acid radical-scavenging capacity assay using a Trolox standard curve as described by Teow et al. (2007).

Primary metabolite profiling by gas chromatography–mass spectrometry

Leaf sampling was performed at midday in the same leaves where gas exchange and antioxidant response characterization were performed (100 mg FW). Metabolite extraction and derivatization from frozen ground leaf material were performed as previously detailed (Lisec et al., 2006). GC–MS data were acquired using an Agilent 7683 series auto-sampler (Agilent Technologies, http://www.home.agilent.com), coupled to an Agilent 6890 gas-chromatograph–Leco Pegasus two time-of-flight mass spectrometer (Leco; http://www.leco.com/). The acquisition parameters were identical to those previously described by Caldana et al. (2011). Chromatograms were exported from Leco CHROMATOF software (v.3.34) and imported into the statistical software framework R (http://www.r-project.org/). Ion extraction, peak detection, retention time alignment, and library searching were obtained using the package TARGETSEARCH (Cuadros-Inostroza et al., 2009). Dataset S1 shows the metadata for the metabolite annotated in this work through this technology.

Respiration and oxygen-isotope fractionation measurements

For respiratory measurements, leaves of plants grown at 15°C and 4°C were harvested after 30 min in the dark and placed in a 3 ml stainless-steel closed cuvette maintained at a constant temperature of 15°C and 4°C, respectively. Air samples were sequentially removed from the cuvette and fed into the mass spectrometer (Delta XPlus; Thermo LCC, Bremen, Germany). Changes in the $^{18}O/^{16}O$ ratios and O concentration were obtained to calculate the O-isotope fractionation and the electron partitioning to the alternative pathway τ_a, as described in Del-Saz et al. (2016). End point fractionation values of both the COP (Δ_c) and AOP (Δ_a) were determined in leaves treated for 30 min with a solution of 25 mM salicylhydroxamic acid and 10 mM potassium cyanide (KCN), respectively ($n = 3$). Values of Δ_a of $32.9 \pm 0.1‰$ and $32.7 \pm 0.3‰$ were obtained for CQ and DC, respectively, and values of Δ_c of $20.9 \pm 0.3‰$ and $20.3 \pm 0.2‰$

were obtained for CQ and DC, respectively. No temperature effects were observed previously for discrimination values of Δ_a (Gonzàlez-Meler *et al.*, 1999; MacFarlane *et al.*, 2009). The individual activities of the COP (v_{cyt}) and AOP (v_{alt}) were calculated as described previously (Del-Saz *et al.*, 2016).

For measurements of the AOP capacity, leaves were incubated in a solution with 10 mM KCN for 30 min. O-uptake rates were measured in darkness using a liquid-phase Clark-type O electrode (Rank Brothers, Cambridge, UK) in a solution containing 30 mM MES pH 6.2 and 0.2 mM calcium chloride. For plants grown at 15°C and 4°C, measurements were performed at a constant temperature of 15°C and 4°C, respectively.

Ionomic extraction and quantification

Leaves and roots from CQ and DC at 4°C and 15°C (four to six biological replicates per species and treatment) were dried at 80°C and subsequently ground to dry powder. Total C and N contents and ionomic quantification (P, potassium, copper, iron, manganese, magnesium, sulphur (S), and zinc) were carried out by CEBAS-CSIC Ionomic Service (Murcia, Spain).

Modelling and statistics

We used the modified Thompson τ technique to check for data outliers in the data sets. ANOVA and Tukey's multiple comparisons test ($P < 0.05$) were performed to assess the effects of the treatments. Pearson correlation analysis was used to determine the correlation between gas-exchange and Chl fluorescence parameters vs biochemical and enzymatic antioxidant activities ($P < 0.05$). Principal component analysis (PCA) was employed to explore the putative correlation of metabolic profiles with treatments and species. Data were previously normalized by the median and then centred and scaled. These analyses were performed using the free software R (2017) with the LATTICE (Deepayan, 2008) and PCAMETHODS libraries (Stacklies *et al.*, 2007). Gas-exchange measurements/primary metabolism and antioxidant biochemistry employed 6–10 and 4–10 biological replicates, respectively.

Metabolites–traits associations

We used a two-step approach based on regularized regression to infer species-dependent associations between the physiological traits and metabolite levels. In the first step, we determined the associations between physiological traits and metabolites that were common to different species by employing least absolute shrinkage and selection operator (LASSO) with fusion penalty (Omranian *et al.*, 2016). The associations common to the species were identified from multiple data sets (metabolite levels and trait scores across different temperatures from multiple species) by imposing two biological constraints modelled as fused LASSO: (1) sparsity of the associations and (2) similarity of associations inferred from individual data sets (species). To this end, every physiological trait was considered as a response and the metabolite levels as predictors (Fig. S1). In the second step, we

determined the residual of each species-dependent data set upon removing the effects common to different species found in the first step. We then inferred the species-dependent associations by again employing LASSO regression on the respective residuals (more details are given in Methods S1).

Results

Low temperature drastically decreased *in vivo* carbon balance in *Colobanthus quitensis*

We investigated the changes in A_N, P_R, and R_{dark} for the different temperature treatments, as it is known that any of these processes could alleviate altered redox status under cold stress (Xiong *et al.*, 1999; Hoermiller *et al.*, 2017; O'Leary *et al.*, 2019). Low temperature (4°C) promoted a significant decrease of A_N and P_R in both ecotypes of CQ (Fig. 2a,b). The population of CQ_A achieved higher A_N and P_R values than CQ_F did at 15°C; however, CQ_F displayed higher P_R at 23°C (Fig. 2b). R_{dark} did not show such a trend; both CQ ecotypes showed high respiration rates up to mean values of 4.6 µmol CO_2 m^{-2} s^{-1} (Fig. 2c). We also examined two independent stress marker parameters (F_v/F_m and lipid peroxidation) to assess the stress level induced by temperature. No differences were observed for F_v/F_m between 15 and 23°C, for which both ecotypes optimal values were obtained (0.76–0.79; Fig. 2d); however, at 4°C no reduction was observed for CQ_A, whereas the Andean ecotype showed a significant decrease (Fig. 2d). Nonphotochemical quenching and lipid peroxidation measurements (used as a proxy of oxidative membrane damage) did not show any particular pattern among different temperature treatments (Fig. 2e,f). We also found that the reference non-Antarctic species DC displayed a significant reduction of gas-exchange parameters, in comparison with the photosynthetic optimum (15°C), as well as the F_v/F_m at low temperature; however, no difference was observed for lipid peroxidation (Fig. 2).

Low temperature (4°C) showed significant stomatal conductance (g_s) reductions of 46–67%, whereas g_m showed even more drastic reductions (75–97%; Table S1) for both species. Indeed, g_m showed reduced values (0.004–0.01 µmol CO_2 m^{-2} s^{-1}) at 4°C, considerably constraining CO_2 availability at the carboxylation sites in the chloroplast (C_c), and thus strongly limiting the potential final photosynthesis (Table S1). Both ecotypes of CQ showed high $V_{c,max}$ reductions (68–73%), and reduction of this parameter in DC was even higher (82%; Table S1). Interestingly, the CQ_A ecotype showed a significant photosynthetic reduction at 23°C (Fig. 2a), driven by significant reductions in g_s and ETR (Table S1). $V_{c,max}$ reached the highest values at 23°C, capturing a different behaviour for CQ and DC as their photosynthesis reaches its optimum at 15°C.

Enzymatic antioxidant activities response to low temperature

To evaluate whether CQ_A displayed a special enzymatic activity profile to deal with oxidative stress without showing damage to the membrane or decrease in F_v/F_m, we examined the effect of
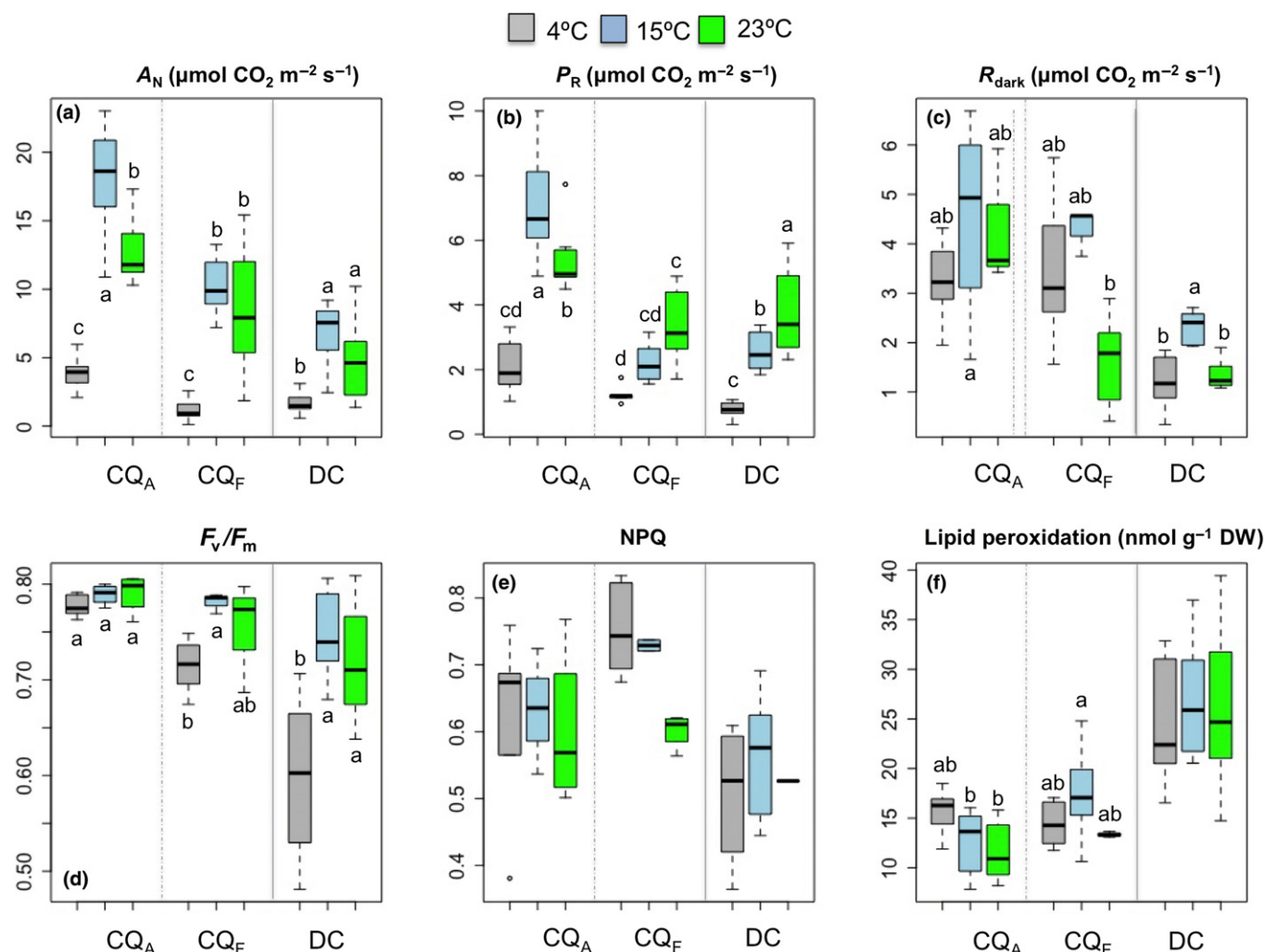
Fig. 2 Box-plots of (a) photosynthesis A_N, (b) photorespiration P_R, (c) respiration R_{dark}, (d) maximal photochemical efficiency of the PSII (F_v/F_m), (e) nonphotochemical quenching (NPQ), and (f) lipid peroxidation measured at 4, 15, and 23°C for both *Colobanthus quitensis* ecotypes, the Antarctic (CQ_A) and the Andean (CQ_F), as well the reference non-Antarctic species *Dianthus chinensis* (DC). Colour indicates the temperature treatment as grey 4°C, blue 15°C, and green 23°C. Vertical dashed lines separate ecotypes; continuous lines separate both species. The bottom and top of the box are the 25th and 75th percentiles (the lower and upper quartiles, respectively), and the band near the middle of the box represents the 50th percentile (the median). The lower and upper whiskers represent, respectively, the minimal and maximal values of the data set. Different letters mean significant differences (per each species) between treatments by Tukey's multiple comparisons' test ($P < 0.05$); no letters indicate no significant differences.

temperature on the activity of the main ROS-scavenging enzymes APX, POX, and CAT (Díaz-Vivancos *et al.*, 2010). First, we found that total soluble protein content (TSP) remains stable in all treatments; surprisingly, however, no significant increases were found for any antioxidant enzyme for CQ ecotypes in response to 4°C in comparison with the optimum at 15°C (Table 1). However, in the non-Antarctic reference species DC both POX and APX activity as well TSP were increased in response to low temperature (Table 1).

Specific primary metabolism associations with physiological responses to temperature treatments

We were able to annotate 87 different metabolites, such as amino acids, sugars, sugar-alcohols, and organic acids (including several

intermediates of the TCA cycle; Dataset S2). Although the chemical identity of several metabolites is currently unknown, they were also considered in the analysis to assess their potential physiological role and to establish putative targets for future studies. To see whether the metabolic signatures can distinguish the genotypes and the different treatments, we conducted PCA. This analysis showed that low temperature (4°C) affected the metabolic profiles of all species studied, whereas almost no differences were observed between plants grown at 15 and 23°C (Fig. S2). A strong metabolic response to 4°C grouped this treatment in the negative extreme of PC1 (59.3% explained variance), whereas plants grown at 15 and 23°C clustered together in more positive values of the same axis (Fig. S2). Moreover, significant variation in the CQ metabolome at 4°C (64.8% and 60.4% of the metabolites significantly increased in CQ_A and CQ_F,

Table 1 Total soluble protein and activities of antioxidant enzymes from plants grown at 4, 15, and 23°C of both ecotypes of *Colobanthus quitensis* (CQ) and *Dianthus chinensis* (DC).

Species	T (°C)	TSP(mg g^{-1} DW)	POX(mmol min^{-1} g^{-1} DW)	CAT(mmol min^{-1} g^{-1} DW)	APX(mmol min^{-1} g^{-1} DW)
CQ$_A$	4	24.9 ± 2.0 a	22.0 ± 1.9 a	2006 ± 261 c	25.0 ± 1.2 bc
CQ$_A$	15	22.1 ± 2.7 a	19.8 ± 2.5 ab	3557 ± 178 ab	33.7 ± 3.5 ab
CQ$_A$	23	29.5 ± 3.6 a	4.5 ± 1.1 d	3508 ± 287 ab	35.3 ± 1.1 a
CQ$_F$	4	33.4 ± 1.4 a	14.8 ± 1.7 bc	2826 ± 92 bc	18.7 ± 1.0 c
CQ$_F$	15	23.5 ± 3.2 a	15.6 ± 1.5 ab	3741 ± 312 ab	20.4 ± 10.4 c
CQ$_F$	23	33.2 ± 2.7 a	8.6 ± 2.0 d	4024 ± 203 a	20.2 ± 1.7 c
DC	4	22.4 ± 1.1 a	21.0 ± 0.6 a	2245 ± 115 a	23.4 ± 0.8 a
DC	15	16.2 ± 2.2 b	7.9 ± 0.8 b	2530 ± 250 a	17.1 ± 0.3 b
DC	23	10.5 ± 0.5 b	6.4 ± 4.0 b	2697 ± 244 a	15.0 ± 0.6 b

Values are the mean ± SE of total soluble protein (TSP) and activities of peroxidase (POX), catalase (CAT), and ascorbate peroxidase (APX). Different letters mean significant differences between treatments within each species by Tukey's multiple comparisons' test ($P < 0.05$). CQ$_A$, *C. quitensis* Antarctic ecotype; CQ$_F$, *C. quitensis* Andean ecotype.

respectively) were observed, and no significant decreases were identified (Fig. 3). Interestingly, CQ$_A$ accumulated several metabolites at 23°C but CQ$_F$ showed the opposite pattern, with slight changes or even strong reductions (Fig. 3). Likewise, DC showed minor accumulation changes compared with CQ (Fig. 3). We observed that secondary metabolite precursors such as benzoate, shikimate, and *p*-coumarate were highly accumulated at 4°C for both species (Fig. 3), with CQ being values much higher than DC values (Table S2).

To further investigate the metabolic interactions driving the observed physiological responses, we applied the fused LASSO modelling approach, whereby we aimed to predict the measured physiological traits (A_N, P_R, R_{dark}, F_v/F_m and TBARS) based on the gathered corresponding metabolic profiles (Figs 4, S3). This approach allows us to tease apart the associations that are common to both species (in both sign and magnitude) as well as additional associations that may differ in sign and magnitude between species (Fig. S1; Methods S1). In doing so, we were able to distinguish metabolic pathways that are altered between species as well as those that are constitutively related to a physiological trait.

We first inferred the species-dependent responses of the CQ (data from both ecotypes) and of the non-Antarctic species DC. The species-dependent associations obtained by the modelling approach on R_{dark} and membrane damage (TBARS) are presented in Fig. 4 (see Fig. S3 for A_N, P_R, and F_v/F_m). From this point, we focus on metabolites with larger regression coefficients; specifically, the species-dependent associations occurring across the Antarctic and the non-Antarctic species, as well as those that belong to well-described metabolic pathways associated with physiological traits. The species-dependent metabolite–trait associations for CQ showed strong, positive associations between A_N and glycine, mannitol, Unknown-03, and Unknown-06 (Fig. S3). Glycine and mannitol were also associated with A_N in DC, although negatively (Fig. S3), indicating a stress response putatively related to photorespiration and polyol metabolism. Our data suggest activation of metabolic pathways related to polyamines (spermidine), secondary metabolism (tryptophan and *p*-hydroxybenzoate), and aspartate (all negatively associated to A_N in CQ but positively correlated to this trait in DC; Fig. S3). We also observed strong, negative associations in CQ between

A_N and ascorbate, methionine, and Unknown-08 (Fig. S3), indicating activation of S metabolism and increase of antioxidant capacity when photosynthesis drops.

Thirteen metabolites showed negative association with P_R in CQ and DC, including pyruvate and two TCA intermediates: fumarate and malate (Fig. S3). Respiration was positively related to secondary metabolism (phenylalanine), polyamines precursors (ornithine and arginine), and S metabolism (methionine), and negative associations with the precursor to S metabolism (cysteine) and polyamines (spermidine). Interestingly, all these metabolic pathways are interconnected by *S*-adenosyl-methionine (AdoMet), which is necessary for the transfer of methyl groups in reactions leading to the synthesis of secondary metabolites and polyamines (Long *et al.*, 2015). We note that methionine showed a negative association with respiration in CQ and DC. By contrast, cysteine was positively related with respiration in CQ but not in DC (Fig. 4).

The models for F_v/F_m and lipid peroxidation showed several metabolites already found for A_N, P_R, and R_{dark} (Figs 4, S3). Interestingly, we also observed associations between these traits and an important number of sugars (trehalose, sucrose, fructose, and arabinose), sugar-alcohols (mannitol and galactinol) and organic acids (*p*-coumarate, benzoate, galacturonic acid, and glucuronic acid), which are typically involved in osmoprotection, signalling, ROS scavenging, membrane stabilization, and/or cell wall remodelling (Figs 4, S3); these findings also suggest strong and differential association between respiration and S, polyamine, and secondary metabolisms in CQ.

High cytochrome respiratory rates and antioxidant capacity characterize the response of *Colobanthus quitensis* to low temperature

To validate the fused LASSO results, we performed two additional experiments where, first, we further characterized the mitochondrial respiration pathways and, second, measured S-containing antioxidant compounds and the total antioxidant capacity. Here, we focused on CQ$_A$ (because this ecotype did not show any physiological damage at low temperature), and we additionally maintained the reference species DC at 4°C (stress
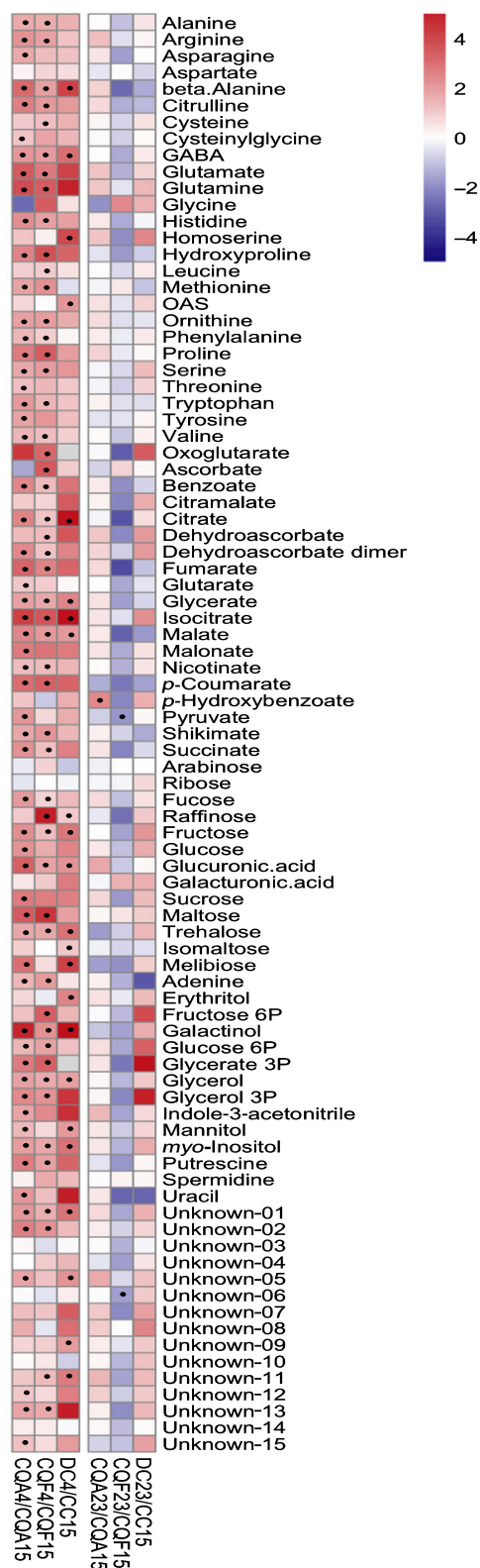
Fig. 3 Metabolic responses to temperature treatments. Heat-map of fold-change for metabolite levels in plants grown at 4 and 23°C compared with the optimum condition for Antarctic species (15°C) *Colobanthus quitensis* ecotypes, the Antarctic (CQ$_A$) and the Andean (CQ$_F$), as well the reference non-Antarctic species *Dianthus chinensis* (DC). Black dots mean significant differences with respect to the reference treatment by Tukey's test ($P < 0.05$).

conditions) and 15°C (optimum conditions), where we found stronger physiological and metabolic changes (Figs 2, 3, S2). Leaf structural (LMA) and physiological indicators (F_v/F_m) were employed to assess whether plants were under similar physiological conditions to those in the previous experiment (Table S3).

To study the role of the two respiratory pathways, COP and AOP, in driving the tolerance to cold, we measured their *in vivo* activities at 4°C and 15°C by using the O isotope fractionation technique (Del-Saz *et al.*, 2018). The results showed that total foliar oxygen respiration V_t decreased significantly (> 50%) at 4°C in the two species, although CQ showed the highest values at both temperatures (Table 2). Electron partitioning to the AOP (τ_a) decreased significantly (61.9%, Table 2) in response to low temperature in CQ but increased in DC (17.8%). The changes in V_t and τ_a at 4°C were due to variations in the *in vivo* activities of COX (v_{cyt}) and AOX (v_{alt}). Both v_{cyt} and v_{alt} significantly decreased in the two species at 4°C compared with 15°C (Table 2). Interestingly, from 15°C to 4°C, CQ showed the lowest and highest reductions in v_{cyt} (49.6%) and v_{alt} (83%), respectively, and it captured the lowest absolute value of v_{alt} (0.43 nmol O$_2$ g^{-1} DW s^{-1}) at 4°C (Table 2). We observed different trends when we measured the capacity of the alternative pathway V_{alt} at 4°C. This parameter was unaffected in DC but significantly increased in CQ (121%; Table 2).

These data confirmed that CQ maintains high respiration rates at 4°C, mainly at the expense of the COP, thus leading to a higher production of ATP per mole of respired O$_2$. Our model suggested that the physiological responses and stress status of CQ are linked to S metabolism, which is largely dependent on ATP (Stephanopoulos, 1998; Long *et al.*, 2015). We therefore determined GSH content, as this is usually the main S-containing nonenzymatic antioxidant; however, the metabolism of GSH did not show significant changes in CQ (Table 3). GSHt significantly increased at 4°C in CQ and DC mainly at the expense of GSH increases; however, the redox state was maintained at the same level in comparison with the optimum conditions (Table 3).

In this sense, we also evaluated the ion content of the tissues as an integrative approach of metabolic changes, as nutrient mobilization from source to storage tissues is described as a stress response for several species (Avila-Ospina *et al.*, 2014). Interestingly, S content was the only ion that increased at 4°C in CQ (Table S4). Taking into account that CQ did not show any oxidative stress symptom at 4°C and its metabolic results indicated increases in secondary metabolism, which could be related to antioxidant capacity, we decided to analyse the total antioxidant capacity of the leaves from plants grown at 4 and 15°C. Fig. 5 shows that CQ leaf tissues displayed an impressive antioxidant capacity (between 13- and 24-fold higher than DC at 4°C and 15°C, respectively). In addition, CQ did not show any increase in the total antioxidant activity at 4°C, thus antioxidant activity is constitutively elevated in CQ (Fig. 5). In agreement with these data, some secondary metabolites and phenolic compound precursors, like benzoic acid, shikimate, and *p*-coumarate, showed higher values in all conditions tested in CQ than in the other species (five- to 10-fold higher) (Fig. 3; Table S2; Dataset S1).
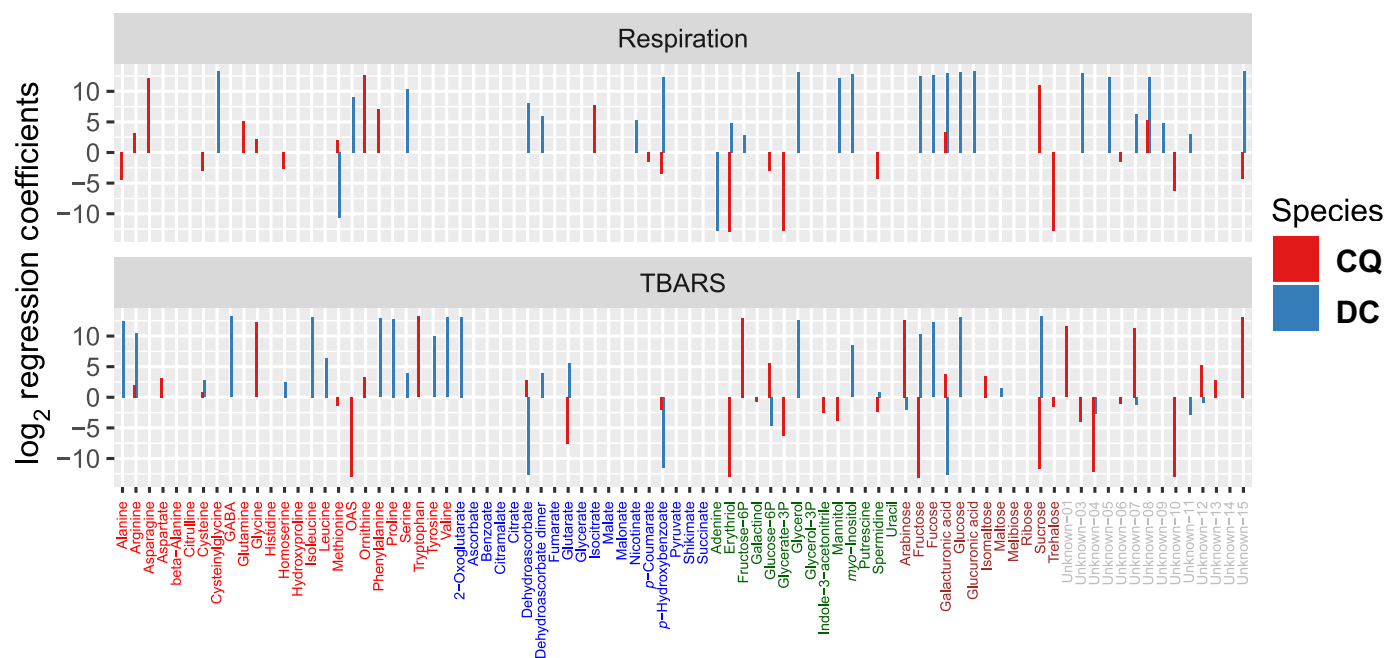
Fig. 4 Species-dependent metabolite–trait associations (*Colobanthus quitensis* (CQ) vs *Dianthus chinensis* (DC)). The bi-sided bar plot of the log$_2$-transformed regression coefficients (associations) between metabolites and the physiological and biochemical parameters respiration (R_{dark}) and thiobarbituric acid-reactive substances (TBARS; lipid peroxidation). The species-dependent metabolite–trait associations were extracted for CQ as well as DC and the absolute values of the regression coefficients were log$_2$ transformed. The metabolites are sorted and coloured based on their chemical classes (red for amino acids, blue for organic acids, green for sugars, brown for 'others', and grey for unknown metabolites).

Discussion

Low temperature reduces carbon balance even in the Antarctic species

CQ is one of the two vascular species that were able to naturally colonize some of the summer ice-free areas in Antarctica, where they have to deal with an extreme environment (Robinson *et al.*, 2003; Cavieres *et al.*, 2016). Interestingly, we observed that CQ commonly does not show any macroscopic stress symptom under natural growth conditions on King George Island (Antarctica) or in the Andean range when we collected it (Fig. 1). These observations agree with results obtained in our experimental setup, where no significant differences were observed for F_v/F_m and lipid peroxidation in CQ grown under the controlled environmental condition at 4°C (Fig. 2).

Photosynthesis is traditionally considered the main energy sink. One of the stress tolerance mechanisms of Antarctic vascular species could be their ability to maintain high A_N at low temperatures, helping them to avoid ROS generation while maintaining productivity and energy status (Xiong *et al.*, 1999; Cavieres *et al.*, 2016). Several studies established that optimal photosynthetic temperatures are correlated with specific adaptations of the main physiological and biochemical drivers (g_s, g_m, and Rubisco), which in turn are tightly linked to the bioclimatic origin of the species (von Caemmerer & Evans, 2015; Xiong *et al.*, 2015; Perdomo *et al.*, 2016). Antarctic plants have photosynthetic optima of *c.* 15–19°C, and at 0°C they maintain up to 30% (under short-term temperature-response curves; Xiong *et al.*, 1999); this is lower than the optima for temperate/tropical species (23–35°C), which commonly show a dramatic decrease at 10–15°C (Yamori *et al.*, 2014). In agreement with previous reports (Cavieres *et al.*, 2016 and references therein), we measured the highest photosynthetic values for CQ at 15°C (Fig. 2). Here, low temperature imposed significant decreases in A_N for both species, indicating that is not

Table 2 Respiration and activities of the cytochromic and alternative pathways measured by oxygen isotope fractionation.

Species	T (°C)	V_t	τ_a	v_{cyt}	v_{alt}	V_{alt}
CQ	4	5.14 ± 0.19*	0.08 ± 0.01*	4.71 ± 0.14*	0.43 ± 0.08*	10.96 ± 2.03*
CQ	15	11.98 ± 1.16	0.21 ± 0.02	9.49 ± 1.04	2.49 ± 0.30	4.97 ± 0.52
DC	4	2.93 ± 0.11*	0.33 ± 0.02*	1.94 ± 0.07*	0.99 ± 0.07*	5.72 ± 0.67
DC	15	5.93 ± 0.23	0.28 ± 0.02	4.27 ± 0.23	1.65 ± 0.08	3.85 ± 0.62

Total respiration V_t (nmol O$_2$ g^{-1} DW s^{-1}), electron partitioning to the alternative pathway τ_a, cytochromic pathway activity v_{cyt} (nmol O$_2$ g^{-1} DW s^{-1}), alternative pathway activity v_{alt} (nmol O$_2$ g^{-1} DW s^{-1}), and alternative pathway capacity V_{alt} (nmol O$_2$ g^{-1} DW s^{-1}) in leaves of *Colobanthus quitensis* (CQ) and *Dianthus chinensis* (DC) plants grown at 4 and 15°C for 12 d. Data are averages $\pm$ SE of four to six biological replicates. Asterisks mean significant differences between both treatments for each species by Tukey's test ($P < 0.05$).

Table 3 Determination of total glutathione and the redox state.

Species	T (°C)	GSHt	GSSG	GSH	Redox state
CQ	4	376.0 ± 76.9*	63.8 ± 9.0	324.9 ± 38.3*	0.86
CQ	15	200.1 ± 40.5	40.5 ± 2.6	170.0 ± 14.8	0.85
DC	4	1196.8 ± 36.5*	104.3 ± 4.7	1118.6 ± 53.7*	0.93
DC	15	963.5 ± 34.3	88.0 ± 12.4	875.8 ± 41.6	0.91

Glutathione content in *Colobanthus quitensis* (CQ) and *Dianthus chinensis* (DC) plants grown at 4 and 15°C. Total glutathione (GSHt), oxidized glutathione (GSSG) and reduced glutathione (GSH) contents are expressed as nmol g^{-1} DW. Redox state is the ratio between GSH and GSHt. Data are averages ± SE of four or five biological replicates. Asterisks mean significant differences between both temperatures for each species by Tukey's test ($P < 0.05$).

their main strategy to avoid ROS formation under long-term cold conditions (Fig. 2).

Photosynthesis at low temperature significantly drops (Fig. 2), mostly driven by a strong reduction in g_m rather than g_s or Rubisco performance (Table S1). This is not surprising, as it has already been shown that g_m is drastically reduced when temperature is decreased, whereas g_s remains comparatively more stable or even increases (Warren & Dreyer, 2006; Yamori *et al.*, 2006; Warren, 2008; von Caemmerer & Evans, 2014). Interestingly, it has been found that Rubisco in CQ showed a high specificity factor for CO_2 ($S_{c/o}$) and k_{cat}^c, probably to alleviate the CO_2 diffusive restrictions at the chloroplast carboxylation sites. Moreover, it has been found that g_m is the most relevant photosynthetic limitation under field conditions and at different temperatures and water availabilities (Sáez *et al.*, 2017, 2018).

It is already known that there is essential cross-talk between photosynthesis, photorespiration, and respiration orchestrated by metabolites that maintains cell redox state in illuminated leaves (Hoefnagel *et al.*, 1998; Raghavendra & Padmasree, 2003; Noguchi & Yoshida, 2008; O'Leary *et al.*, 2019). Under stress, energy excess in the photosynthetic apparatus may induce respiration to modulate its activity to dissipate redox equivalents from

chloroplasts, helping to orchestrate a readjustment of redox homeostasis (Voss *et al.*, 2013; Florez-Sarasa *et al.*, 2016; Del-Saz *et al.*, 2018). Moreover, it has been described that respiration may provide ATP for oxidation of excess redox equivalents in chloroplasts (Tezara *et al.*, 2008). Remarkably, respiration was mostly unaffected by the temperature treatments, indicating an important robustness and acclimation of this parameter to low temperature. We observed high respiration rates for CQ, which were also demonstrated in previous studies (Xiong *et al.*, 1999; Sáez *et al.*, 2017). Indeed, the respiration rates for CQ are in the upper range when compared with a global dataset from 899 species (Atkin *et al.*, 2015). We observed that low temperature decreases V_t, as reviewed in Heidarvand *et al.* (2017), and there is a different behaviour in the *in vivo* activities of the two respiratory pathways as well as in V_{alt}. CQ showed a higher reduction in V_t and v_{alt} than DC did, in spite of the strong increase observed in V_{alt}. Comparatively, CQ maintained a constitutively elevated COP; thus, ATP was synthesized even under low temperature, but without increasing the activity of AOX (even having enough capacity to increase it) (Table 2). This is in line with previous studies that reported higher abundance of AOX protein during seasonal acclimation of respiration in alpine grasses (Searle *et al.*,
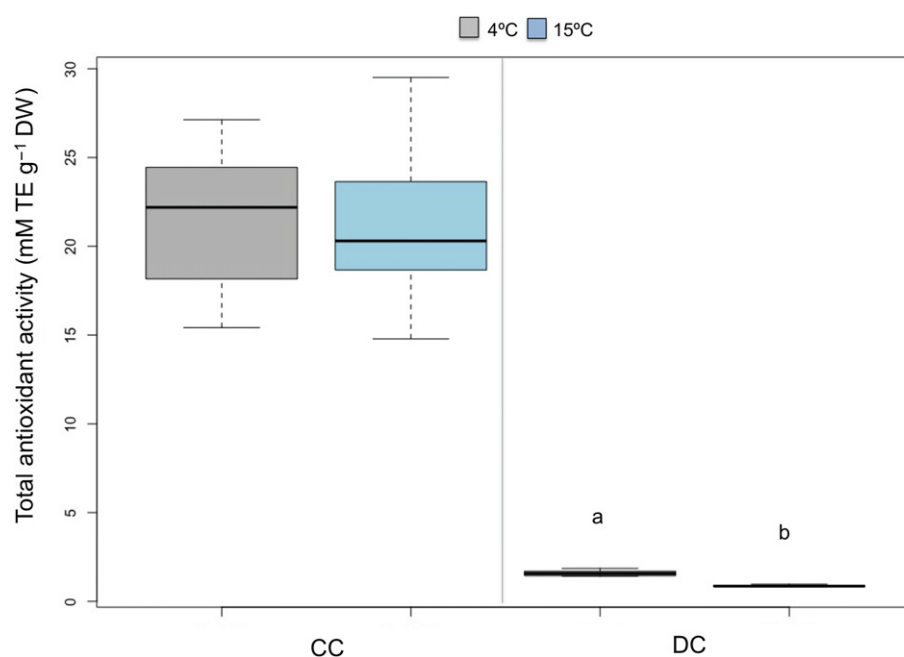

Fig. 5 Total antioxidant capacity of leaves (mM Trolox equivalent (TE) g^{-1} DW) from *Colobanthus quitensis* (CQ) and *Dianthus chinensis* (DC) grown at 4 and 15°C. Data are averages ± SE of four or five biological replicates. The bottom and top of a box are the 25th and 75th percentiles (the lower and upper quartiles, respectively), and the band near the middle of the box represents the 50th percentile (the median). The lower and upper whiskers represent, respectively, the minimal and maximal values of the data set. Different letters mean significant differences (per each species) between treatments by Tukey's multiple comparisons' test ($P < 0.05$); no letters indicate no significant differences.

2011). Despite the effect of low temperature in decreasing the rate of respiration in CQ, its response is the most appropriate to maximize both the respiratory energy efficiency and synthesis of ATP via the COP, similar to that observed in *Betula nana* (Kornfeld *et al.*, 2013). Thus, ATP can be supplied from mitochondria to compensate for decreased rates of chloroplast ATP synthesis under stress (Tezara *et al.*, 2008; Atkin & Macherel, 2009). Moreover, this response provides AOP with flexibility to deal with possible redox impairment.

Fightback: an integrated perspective of the stress tolerance strategies operating in *Colobanthus quitensis*

There were no remarkable changes in the activities of antioxidant enzymes at 4°C compared with 15°C (Table 1), in agreement with previous studies under high light and low temperature stressful conditions (Pérez-Torres *et al.*, 2004a). Another putative defence strategy displayed by CQ could be the accumulation of nonenzymatic antioxidants, such as carbohydrates and proline. Consistently, our results showed both a large metabolite accumulation in response to 4°C (Fig. 3) and a huge constitutive antioxidant capacity (Fig. 5) higher than in the DC data and as well another published data in several species in the literature, including the other Antarctic vascular plant *Deschampsia antarctica* (Benavente-García *et al.*, 2000; Pérez-Torres *et al.*, 2004b; Teow *et al.*, 2007). Thus, when photosynthesis and photorespiration are constrained under low temperatures, N and S metabolism could play an important role in cell homeostasis by consuming energy (ATP), reducing equivalents (NADPH) and C skeletons produced by the TCA cycle (Stephanopoulos, 1998; Nunes-Nesi *et al.*, 2010; Bloom, 2015; Long *et al.*, 2015).

Metabolic association to diverse physiological responses, from biomass to photosynthesis, stomatal or mesophyll conductance, was previously employed to screen the possible metabolic pathways associated to these processes with the proper statistical modelling (Sulpice *et al.*, 2013; Gago *et al.*, 2016; de Abreu e Lima *et al.*, 2017, 2018). The fused LASSO approach has been used previously in reconstruction of gene regulatory networks across multiple conditions (Omranian *et al.*, 2016), extraction of conserved gene regulatory networks (Lam *et al.*, 2016), and inferring condition-specific gene regulatory networks (Deng *et al.*, 2018; Lyu *et al.*, 2018). Here, investigating the species-dependent associations allows us to identify key regulators of physiological responses in a particular species that would otherwise not be possible by considering differential correlation analysis (de la Fuente, 2010).

Fig. 6 shows the main metabolic pathways, including metabolites associated with respiration in the species-dependent fused LASSO model for CQ. This diagram also includes information obtained with subsequent experiments to provide an integrated picture of the putative mechanisms operating in this species to cope with cold conditions. CQ and DC accumulated several metabolites at 4°C (Fig. 3), which could be attributed to increased synthesis, decreased degradation, and/or reduced export to sink tissues (mainly roots). Accumulation of amino acids does not seem to result from protein degradation, as protein levels

were unaltered or even slightly increased at 4°C (Table 1). Numerous metabolites were linked to physiological traits by the models (Figs 4, S3). In particular, species-dependent models for CQ included associations between S metabolism, polyamines, and aromatic amino acids with the physiological traits studied (Figs 4, 6); by contrast, we did not observe such strong associations in DC (Fig. 4). It has been estimated that 80% of the methionine pool is used for the synthesis of AdoMet, an essential metabolite for the biosynthesis of lipids (phosphatidylcholine, the major polar lipid associated with cell membranes; Ravanel *et al.*, 1998) and polyamines (Long *et al.*, 2015). In agreement with these observations, the nutrient mobilization from leaves to storage tissues under stressful conditions is frequently reported in several species (Avila-Ospina *et al.*, 2014); however, CQ grown at 4°C followed the contrary pattern, even showing a significant increase in the leaves' S content compared with the ones grown at 15°C (Table S4).

Biosynthesis of S-containing compounds implies important requirements in terms of energy and reducing equivalents (Stephanopoulos, 1998; Long *et al.*, 2015). Reduction of sulphate to sulphide consumes $732\ kJ\ mol^{-1}$, whereas nitrate assimilation requires $478\ kJ\ mol^{-1}$. The ATP and NADPH required for sulphate assimilation in green tissues are largely met by photosynthesis. In nonphotosynthetic tissues, energy and reducing power are provided by respiration and the reductive pentose-phosphate pathway, respectively (Long *et al.*, 2015). The synthesis of methionine is the most expensive in terms of moles of ATP consumed. A recent computational calculation showed that glucose-fed *Escherichia coli* require 18 ATP molecules to produce one molecule of methionine, assuming that the energy content of NADPH is twice that of ATP (Kaleta *et al.*, 2013). Considering the costs of sulphate reduction and cysteine synthesis (but leaving aside the costs associated with GSH synthesis, as GSH levels were not too high in CQ), plants require three ATP molecules and six NADPH molecules (the energy equivalent to 15 ATP molecules) to synthesize methionine from aspartate (Long *et al.*, 2015), a similar cost to that calculated for *E. coli* (Kaleta *et al.*, 2013).

Also, the synthesis of flavonols/phenylpropanoids from phenylalanine demands large amounts of energy and reducing power (Saito *et al.*, 2013). Indeed, it has been suggested that synthesis of phenolic metabolites could help to alleviate the surplus of NADPH when photosynthesis decreases (Akhtar *et al.*, 2010; Selmar & Kleinwächter, 2013; Caretto *et al.*, 2015). Interestingly, CQ showed higher levels of shikimate, benzoate, and hydroxycinnamic acid than DC did (Table S2). The phenylpropanoid–acetate pathway is the main metabolic route for the production of flavonoids. We speculate that CQ invests large amounts of C and energy to synthesize these compounds because flavonoids are important for reducing the negative effects of ultraviolet radiation (Long *et al.*, 2015), which is particularly important due to the high irradiances found in Antarctica and the Andes. The synthesis of naringenin (a hub metabolite for the biosynthesis of multiple flavonoids) from phosphoenolpyruvate and erythrose 4-phosphate consumes energy equivalent to 10 ATP molecules. This is a conservative calculation, because naringenin is just an
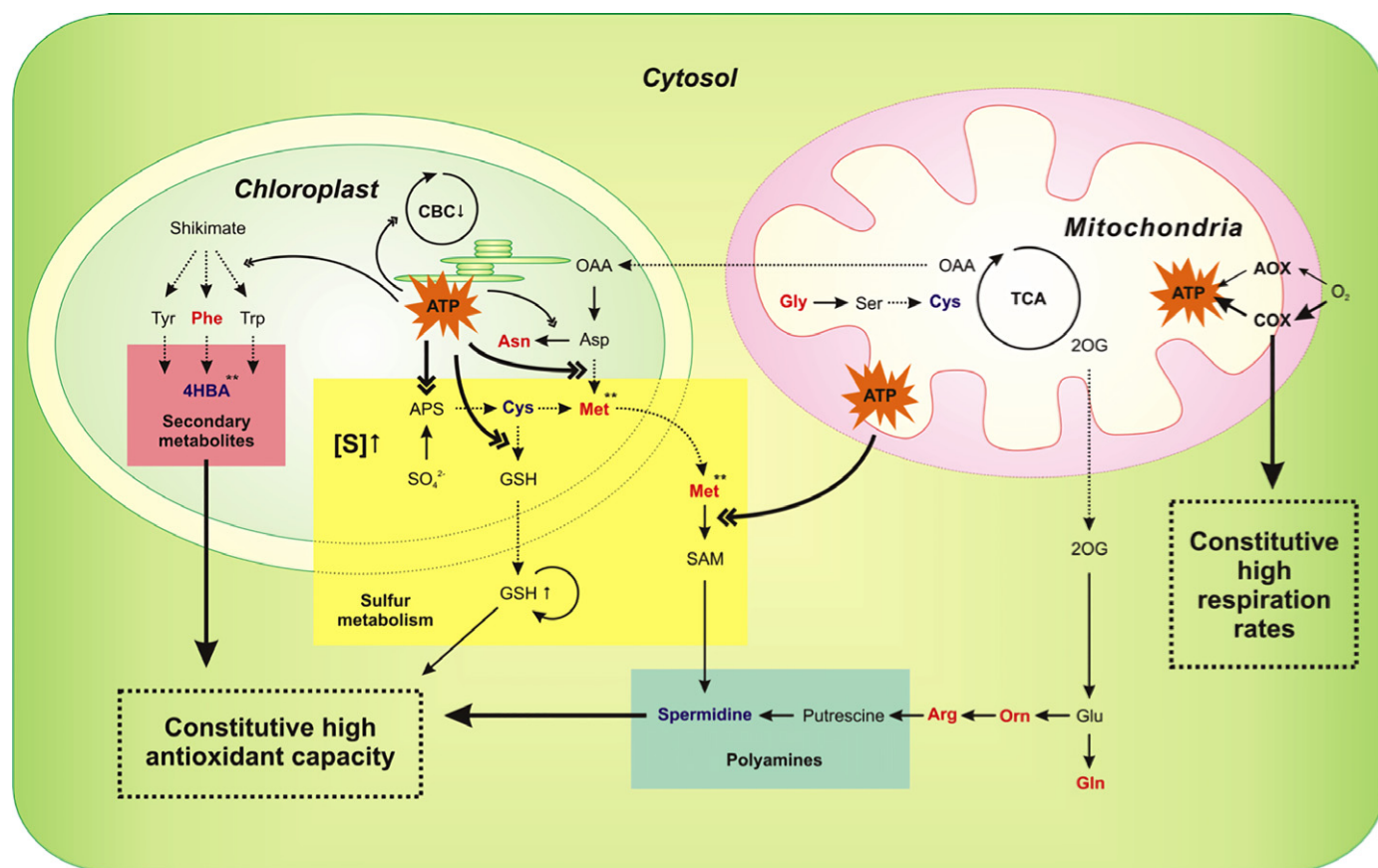
Fig. 6 Integrative model for *Colobanthus quitensis* response under cold temperature. Significant metabolites and main biochemical pathways associated by fused LASSO approach with mitochondrial respiration are shown. Physiological responses are also integrated in the model as the respiratory cytochrome oxidase pathway and alternative oxidase pathway, energy production (ATP), in coordination with antioxidant biochemical strategy linked to glutathione synthesis and activity and total antioxidant tissue capacity. Blue and red colours indicate positive and negative relationship observed by the fused LASSO models; * or ** signal a common metabolite between the Antarctic and the model species with the same or inverse relationship, respectively. 2-OG, 2-oxoglutarate; 4-HBA, 4-hydroxybenzoic acid; AOX, alternative oxidase; APS, adenosine-5′-phosphosulphate; CBC, Calvin–Benson cycle; COX, cytochrome c oxidase; GSH, glutathione; OAA, oxaloacetate; SAM, *S*-adenosyl-L-methionine.

intermediate. It is important to note that AdoMet is also necessary for the multiple methylation reactions leading to different flavonoids (Long *et al.*, 2015), which highlights the importance of S metabolism in this species.

Conclusions

Altogether, our results suggest that this species invests an important amount of resources to produce 'expensive' compounds, such as S-containing and secondary metabolites. These results nicely fit with the constitutive high antioxidant capacity and elevated V_t and v_{cyt} measured in CQ (Fig. 5; Table 2). A deeper characterization of the mitochondrial respiratory pathways in CQ showed notable v_{cyt} rates, thus ensuring mitochondrial ATP production at low temperature. Also, CQ's antioxidant capacity (not driven by ROS-removal enzymes, ascorbate or GSH) was several times higher than that measured on the reference non-Antarctic species DC. Thus, long-term stress tolerance mechanisms in CQ seem to be sustained by complex and energy-costly S-based molecules, polyamines, and secondary metabolites to deal with one of the most extreme environments on Earth, Antarctica.

ORCID

Lohengrin Cavieres https://orcid.org/0000-0001-9122-3020
Alisdair Fernie https://orcid.org/0000-0001-9000-335X
Jorge Gago https://orcid.org/0000-0002-4293-0105

References

de Abreu e Lima F, Li K, Wen W, Yan J, Nikoloski Z, Willmitzer L, Brotman Y. 2018. Unraveling lipid metabolism in maize with time-resolved multi-omics data. *The Plant Journal* 93: 1102–1115.

de Abreu e Lima F, Westhues M, Cuadros-Inostroza Á, Willmitzer L, Melchinger AE, Nikoloski Z. 2017. Metabolic robustness in young roots underpins a predictive model of maize hybrid performance in the field. *The Plant Journal* 90: 319–329.

Akhtar TA, Lees HA, Lampi MA, Enstone D, Brain RA, Greenberg BM. 2010. Photosynthetic redox imbalance influences flavonoid biosynthesis in *Lemna gibba*. *Plant, Cell & Environment* 33: 1205–1219.

Angiel PJ, Potocki M, Biszczuk-Jakubowska J. 2010. Weather condition characteristics at the H. Arctowski station (South Shetlands, Antarctica) for 2006, in comparison with multi-year research results. *Miscellanea Geographica* 14: 79–89.

Araújo WL, Nunes-Nesi A, Osorio S, Usadel B, Fuentes D, Nagy R, Balbo I, Lehmann M, Studart-Witkowski C, Tohge T *et al.* 2011. Antisense inhibition of the iron–sulphur subunit of succinate dehydrogenase enhances photosynthesis and growth in tomato via an organic acid-mediated effect on stomatal aperture. *Plant Cell* 23: 600–627.

Araújo WL, Tohge T, Osorio S, Lohse M, Balbo I, Krahnert I, Sienkiewicz-Porzucek A, Usadel B, Nunes-Nesi A, Fernie AR. 2012. Antisense inhibition of the 2-oxoglutarate dehydrogenase complex in tomato demonstrates its importance for plant respiration and during leaf senescence and fruit maturation. *Plant Cell* 24: 2328–2351.

Arroyo K, Cavieres L, Castor C, Humaña M. 1999. Persistent soil seed bank and standing vegetation at a high alpine site in the central Chilean Andes. *Oecologia* 119: 126–132.

Atkin OK, Bloomfield KJ, Reich PB, Tjoelker MG, Asner GP, Bonal D, Bönisch G, Bradford M, Cernusak LA, Cosio EG. 2015. Global variability in leaf respiration in relation to climate, plant functional types and leaf traits. *New Phytologist* 206: 614–636.

Atkin OK, Macherel D. 2009. The crucial role of plant mitochondria in orchestrating drought tolerance. *Annals of Botany* 103: 581–597.

Atkin OK, Tjoelker MG. 2003. Thermal acclimation and the dynamic response of plant respiration to temperature. *Trends in Plant Science* 8: 343–351.

Avila-Ospina L, Moison M, Yoshimoto K, Masclaux-Daubresse C. 2014. Autophagy, plant senescence, and nutrient recycling. *Journal of Experimental Botany* 65: 3799–3811.

Benavente-García O, Castillo J, Lorente J, Ortuño ADRJ. 2000. Antioxidant activity of phenolics from *Olea europaea* L. leaves. *Food Chemistry* 68: 457–462.

Bloom AJ. 2015. Photorespiration and nitrate assimilation: a major intersection between plant carbon and nitrogen. *Photosynthesis Research* 123: 117–128. doi: 10.1007/s11120-014-0056-y.

Bradford MM. 1976. A rapid and sensitive method for the quantitation of microgram quantities of protein utilizing the principle of protein-dye binding. *Anal Biochem* 72: 248–254.

Bramley-Alves J, King DH, Robinson SA, Miller RE. 2014. *Dominating the antarctic environment: Bryophytes in a time of change*. Dordrecht, the Netherlands: Springer, 309–324.

Brunetti C, George RM, Tattini M, Field K, Davey MP. 2013. Metabolomics in plant environmental physiology. *Journal of Experimental Botany* 64: 4011–4020.

Von Caemmerer S. 2000. *Biochemical models of leaf photosynthesis*. Collingwood, Australia: Csiro Publishing.

von Caemmerer S, Evans JR. 2014. Temperature responses of mesophyll conductance differ greatly between species. *Plant, Cell & Environment* 38: 629–637.

von Caemmerer S, Evans JR. 2015. Temperature responses of mesophyll conductance differ greatly between species. *Plant, Cell & Environment* 38: 629–637.

Cakmak I, Horst WJ. 1991. Effect of aluminium on lipid peroxidation, superoxide dismutase, catalase, and peroxidase activities in root tips of soybean (*Glycine max*). *Physiologia Plantarum* 83: 463–468.

Caldana C, Degenkolbe T, Cuadros-Inostroza A, Klie S, Sulpice R, Leisse A, Steinhauser D, Fernie AR, Willmitzer L, Hannah MA. 2011. High-density kinetic analysis of the metabolomic and transcriptomic response of Arabidopsis to eight environmental conditions. *The Plant Journal* 67: 869–884.

Caretto S, Linsalata V, Colella G, Mita G, Lattanzio V. 2015. Carbon fluxes between primary metabolism and phenolic pathway in plant tissues under stress. *International Journal of Molecular Sciences* 16: 26378–26394.

Casanova-Katny MA, Bravo LA, Molina-Montenegro M, Corcuera LJ, Cavieres LA. 2006. Photosynthetic performance of *Colobanthus quitensis* (Kunth) Bartl. (Caryophyllaceae) in a high-elevation site of the Andes of central Chile. *Revista Chilena de Historia Natural* 79: 41–53.

Cavieres LA, Badano EI, Sierra-Almeida A, Molina-Montenegro MA. 2007. Microclimatic modifications of cushion plants and their consequences for seedling survival of native and non-native herbaceous species in the high Andes of central Chile. *Arctic, Antarctic, and Alpine Research* 39: 229–236.

Cavieres LA, Sáez P, Sanhueza C, Sierra-Almeida A, Rabert C, Corcuera LJ, Alberdi M, Bravo LA. 2016. Ecophysiological traits of Antarctic vascular plants: their importance in the responses to climate change. *Plant Ecology* 217: 343–358.

Clemente-Moreno MJ, Diaz-Vivancos P, Rubio M, Fernandez N, Hernández JA. 2013. Chloroplast protection in Plum Pox Virus-infected peach plants by l-2-oxo-4-thiazolidine-carboxylic acid treatments: effect in the proteome. *Plant, Cell & Environment* 36: 640–654.

Cuadros-Inostroza A, Caldana C, Redestig H, Kusano M, Lisec J, Peña-Cortés H, Willmitzer L, Hannah MA. 2009. TargetSearch – a Bioconductor package for the efficient preprocessing of GC–MS metabolite profiling data. *BMC Bioinformatics* 10: 1–12. e428

Deepayan S. 2008. *Lattice: Multivariate data visualization with R*. New York, NY: Springer.

Del-Saz NF, Florez-Sarasa I, Clemente-Moreno MJ, Mhadhbi H, Flexas J, Fernie AR, Ribas-Carbó M. 2016. Salinity tolerance is related to cyanide-resistant alternative respiration in *Medicago truncatula* under sudden severe stress. *Plant, Cell & Environment* 39: 2361–2369.

Del-Saz NF, Ribas-Carbo M, McDonald AE, Lambers H, Fernie AR, Florez-Sarasa I. 2018. An *in vivo* perspective of the role(s) of the alternative oxidase pathway. *Trends in Plant Science* 23: 206–219.

Deng W, Zhang K, Liu S, Zhao P, Xu S, Wei H. 2018. JRMGRN: joint reconstruction of multiple gene regulatory networks with common hub genes using data from multiple tissues or conditions. *Bioinformatics* 34: 3470–3478.

Díaz-Vivancos P, Rubio M, Mesonero V, Periago PM, Ros Barceló A, Martínez-Gómez P, Hernández JA. 2006. The apoplastic antioxidant system in Prunus: response to Plum pox virus. *Journal of Experimental Botany* 57: 3813–3824.

Díaz-Vivancos P, Clemente-Moreno MJ, Rubio M, Olmos E, Garcia JA, Martinez-Gomez P, Hernandez JA. 2008. Alteration in the chloroplastic metabolism leads to ROS accumulation in pea plants in response to Plum pox virus. *Journal of Experimental Botany* 59: 2147–2160.

Díaz-Vivancos P, Barba-Espín G, Clemente-Moreno MJ, Hernández JA. 2010. Characterization of the antioxidant system during the vegetative development of pea plants. *Biologia Plantarum* 54: 76–82.

Farquhar GD, Von Caemmerer S, Berry J. 1980. A biochemical model of photosynthetic CO_2 assimilation in leaves of C_3 species. *Planta* 149: 78–90.

Flexas J, Díaz-Espejo A, Berry JA, Cifre J, Galmés J, Kaldenhoff R, Medrano H, Ribas-Carbó M. 2007. Analysis of leakage in IRGA's leaf chambers of open gas exchange systems: quantification and its effects in photosynthesis parameterization. *Journal of Experimental Botany* 58: 1533–1543.

Flexas J, Gago J. 2018. A role for ecophysiology in the 'omics' era. *The Plant Journal* 96: 251–259.

Florez-Sarasa I, Ribas-Carbo M, Del-Saz NF, Schwahn K, Nikoloski Z, Fernie AR, Flexas J. 2016. Unravelling the *in vivo* regulation and metabolic role of the alternative oxidase pathway in C_3 species under photoinhibitory conditions. *New Phytologist* 212: 66–79.

Fu X, Ning G, Gao L, Bao M. 2008. Genetic diversity of Dianthus accessions as assessedusing two molecular marker systems (SRAPs and ISSRs) and morphological traits. *Scientia Horticulturae* 117: 263–270.

de la Fuente A. 2010. From 'differential expression' to 'differential networking' – identification of dysfunctional regulatory networks in diseases. *Trends in Genetics* 26: 326–333.

Gago J, Daloso DM, Figueroa CM, Flexas J, Fernie AR, Nikoloski Z. 2016. Relationships of leaf net photosynthesis, stomatal conductance, and mesophyll conductance to primary metabolism: a multispecies meta-analysis approach. *Plant Physiology* 171: 265–279.

Gago J, Fernie AR, Nikoloski Z, Tohge T, Martorell S, Escalona JM, Ribas-Carbó M, Flexas J, Medrano H. 2017. Integrative field scale phenotyping for investigating metabolic components of water stress within a vineyard. *Plant Methods* 13: e90.

Gonzàlez-Meler MA, Ribas-Carbo M, Giles L, Siedow JN. 1999. The effect of growth and measurement temperature on the activity of the alternative respiratory pathway. *Plant Physiology* 120: 765–772.

Harley PC, Loreto F, Di Marco G, Sharkey TD. 1992. Theoretical considerations when estimating the mesophyll conductance to CO_2 flux by analysis of the response of photosynthesis to CO_2. *Plant Physiology* 98: 1429–1436.

Heidarvand L, Millar AH, Taylor NL. 2017. Responses of the mitochondrial respiratory system to low temperature in plants. *Critical Reviews in Plant Sciences* 36: 217–240.

Hoefnagel MHN, Atkin OK, Wiskich JT. 1998. Interdependence between chloroplasts and mitochondria in the light and the dark. *Biochimica et Biophysica Acta – Bioenergetics* 1366: 235–255.

Hoermiller II, Naegele T, Augustin H, Stutz S, Weckwerth W, Heyer AG. 2017. Subcellular reprogramming of metabolism during cold acclimation in *Arabidopsis thaliana*. *Plant, Cell & Environment* 40: 602–610.

Kaleta C, Schäuble S, Rinas U, Schuster S. 2013. Metabolic costs of amino acid and protein production in *Escherichia coli*. *Biotechnology Journal* 8: 1105–1114.

Kappen L. 1999. Pflanzen und Mikroorganismen in der Polar regionen. 30 Jahre deutsche Beitrage zur Polarforschung. *Naturwissenchaften Rundschau* 52: 174–183.

Kornfeld A, Heskel M, Atkin OK, Gough L, Griffin KL, Horton TW, Turnbull MH. 2013. Respiratory flexibility and efficiency are affected by simulated global change in Arctic plants. *New Phytologist* 197: 1161–1172.

Lam KY, Westrick ZM, Müller CL, Christiaen L, Bonneau R. 2016. Fused regression for multi-source gene regulatory network inference. *PLoS Computational Biology* 12: e1005157.

Li Z, Omranian N, Neumetzler L, Wang T, Herter T, Usadel B, Demura T, Giavalisco P, Nikoloski Z, Persson S. 2016. A transcriptional and metabolic framework for secondary wall formation in Arabidopsis. *Plant Physiology* 172: 1334–1351.

Lisec J, Schauer N, Kopka J, Willmitzer L, Fernie AR. 2006. Gas chromatography mass spectrometry-based metabolite profiling in plants. *Nature Protocols* 1: 387–396.

Long SR, Kahn M, Seefeldt L, Tsay Y-F, Kopriva S. 2015. Nitrogen and sulfur. In: Buchanan BB, Gruissem W, Jones RL, eds. *Biochemistry and molecular biology of plants, 2nd edn*. Chichester, UK: John Wiley & Sons.

Lyu Y, Xue L, Zhang F, Koch H, Saba L, Kechris K. 2018. Condition-adaptive fused graphical lasso (CFGL): an adaptive procedure for inferring condition-specific gene co-expression network. *PLoS Computational Biology* 14: e1006436.

MacFarlane C, Hansen LD, Florez-Sarasa I, Ribas-Carbo M. 2009. Plant mitochondria electron partitioning is independent of short-term temperature changes. *Plant, Cell & Environment* 32: 585–591.

Niinemets U, Cescatti A, Rodeghiero M, Tosens T. 2005. Leaf internal diffusion conductance limits photosynthesis more strongly in older leaves of Mediterranean evergreen broad-leaved species. *Plant, Cell & Environment* 28: 1552–1566.

Noguchi K, Yoshida K. 2008. Interaction between photosynthesis and respiration in illuminated leaves. *Mitochondrion* 8: 87–99.

Nunes-Nesi A, Fernie AR, Stitt M. 2010. Metabolic and signaling aspects underpinning the regulation of plant carbon nitrogen interactions. *Molecular Plant* 3: 973–996.

Obata T, Fernie AR. 2012. The use of metabolomics to dissect plant responses to abiotic stresses. *Cellular and Molecular Life Sciences: CMLS* 69: 3225–3243.

O'Leary BM, Asao S, Millar AH, Atkin OK. 2019. Core principles which explain variation in respiration across biological scales. *New Phytologist* 222: 670–686.

Omranian N, Eloundou-Mbebi JMO, Mueller-Roeber B, Nikoloski Z. 2016. Gene regulatory network inference using fused LASSO on multiple data sets. *Scientific Reports* 6: e20533.

Perdomo JA, Carmo-Silva E, Hermida-Carrera C, Flexas J, Galmés J. 2016. Acclimation of biochemical and diffusive components of photosynthesis in rice, wheat, and maize to heat and water deficit: implications for modeling photosynthesis. *Frontiers in Plant Science* 7: 1–16.

Pérez-Torres E, Dinamarca J, Bravo LA, Corcuera LJ. 2004a. Responses of *Colobanthus quitensis* (Kunth) Bartl. to high light and low temperature. *Polar Biology* 27: 183–189.

Pérez-Torres E, García A, Dinamarca J, Alberdi M, Gutiérrez A, Gidekel M, Ivanov AG, Hüner NPA, Corcuera LJ, Bravo LA. 2004b. The role of photochemical quenching and antioxidants in photoprotection of *Deschampsia antarctica*. *Functional Plant Biology* 31: 731–741.

Raghavendra AS, Padmasree K. 2003. Beneficial interactions of mitochondrial metabolism with photosynthetic carbon assimilation. *Trends in Plant Science* 8: 546–553.

Ravanel S, Gakiere B, Job D, Douce R. 1998. The specific features of methionine biosynthesis and metabolism in plants. *Proceedings of the National Academy of Sciences, USA* 95: 7805–7812.

Ribas-Carbó M, Aroca R, Gonza MA, Jose J, Sa M, California MR. 2000. The electron partitioning between the cytochrome and alternative respiratory pathways during chilling recovery in two cultivars of maize differing in chilling sensitivity. *Plant Physiology* 122: 199–204.

Robinson SA, Wasley J, Tobin AK. 2003. Living on the edge – plants and global change in continental and maritime Antarctica. *Global Change Biology* 9: 1681–1717.

Sáez PL, Bravo LA, Cavieres LA, Vallejos V, Sanhueza C, Font-Carrascosa M, Gil-Pelegrín E, Javier Peguero-Pina J, Galmés J. 2017. Photosynthetic limitations in two Antarctic vascular plants: importance of leaf anatomical traits and Rubisco kinetic parameters. *Journal of Experimental Botany* 68: 2871–2883.

Sáez PL, Galmés J, Ramírez CF, Poblete L, Rivera BK, Cavieres LA, Clemente-Moreno MJ, Flexas J, Bravo LA. 2018. Mesophyll conductance to CO_2 is the most significant limitation to photosynthesis at different temperatures and water availabilities in Antarctic vascular species. *Environmental and Experimental Botany* 156: 279–287.

Saito K, Yonekura-Sakakibara K, Nakabayashi R, Higashi Y, Yamazaki M, Tohge T, Fernie AR. 2013. The flavonoid biosynthetic pathway in Arabidopsis: structural and genetic diversity. *Plant Physiology and Biochemistry* 72: 21–34.

Searle SY, Thomas S, Griffin KL, Horton T, Kornfeld A, Yakir D, Hurry V, Turnbull MH. 2011. Leaf respiration and alternative oxidase in field-grown alpine grasses respond to natural changes in temperature and light. *New Phytologist* 189: 1027–1039.

Selmar D, Kleinwächter M. 2013. Stress enhances the synthesis of secondary plant products: the impact of stress-related over-reduction on the accumulation of natural products. *Plant and Cell Physiology* 54: 817–826.

Stacklies W, Redestig H, Scholz M, Walther D, Selbig J. 2007. PCAMethods – A Bioconductor package providing PCA methods for incomplete data. *Bioinformatics* 23: 1164–1167.

Stephanopoulos G. 1998. Metabolic engineering. *Biotechnology and Bioengineering* 58: 119–120.

Sulpice R, Nikoloski Z, Tschoep H, Antonio C, Kleessen S, Larhlimi A, Selbig J, Ishihara H, Gibon Y, Fernie AR *et al*. 2013. Impact of the carbon and nitrogen supply on relationships and connectivity between metabolism and biomass in a broad panel of Arabidopsis accessions. *Plant Physiology* 162: 347–363.

Teow CC, Truong V-D, McFeeters RF, Thompson RL, Pecota KV, Yencho GC. 2007. Antioxidant activities, phenolic and β-carotene contents of sweet potato genotypes with varying flesh colours. *Food Chemistry* 103: 829–838.

Tezara W, Driscoll S, Lawlor DW. 2008. Partitioning of photosynthetic electron flow between CO_2 assimilation and O_2 reduction in sunflower plants under water deficit. *Photosynthetica* 46: 127–134.

Tosens T, Nishida K, Gago J, Coopman RE, Cabrera HM, Carriquí M, Laanisto L, Morales L, Nadal M, Rojas R *et al*. 2016. The photosynthetic capacity in 35 ferns and fern allies: mesophyll CO_2 diffusion as a key trait. *New Phytologist* 209: 1576–1590.

Valentini R, Epron D, De Angelis P, Matteucci G, Dreyer E. 1995. *In situ* estimation of net CO_2 assimilation, photosynthetic electron flow and photorespiration in Turkey oak (*Q. cerris* L.) leaves: diurnal cycles under different levels of water supply. *Plant, Cell & Environment* 18: 631–640.

Voss I, Sunil B, Scheibe R, Raghavendra AS. 2013. Emerging concept for the role of photorespiration as an important part of abiotic stress response. *Plant Biology* 15: 713–722.

Warren CR. 2008. Soil water deficits decrease the internal conductance to CO_2 transfer but atmospheric water deficits do not. *Journal of Experimental Botany* 59: 327–334.

Warren CR, Dreyer E. 2006. Temperature response of photosynthesis and internal conductance to CO_2: results from two independent approaches. *Journal of Experimental Botany* 57: 3057–3067.

Watanabe CK, Hachiya T, Terashima I, Noguchi K. 2008. The lack of alternative oxidase at low temperature leads to a disruption of the balance in carbon and nitrogen metabolism, and to an up-regulation of antioxidant defence systems in *Arabidopsis thaliana* leaves. *Plant, Cell & Environment* 31: 1190–1202.

Wen W, Li K, Alseek S, Omranian N, Zhao L, Zhou Y, Xiao Y, Jin M, Yang N, Liu H *et al*. 2015. Genetic determinants of the network of primary metabolism and their relationships to plant performance in a maize recombinant inbred line population. *Plant Cell* 27: 1839–1856.

Whittaker RH. 1975. *Communities and Ecosystems*. New York: MacMillan Publishing Company Inc.

Xiong D, Liu X, Liu L, Douthe C, Li Y, Peng S, Huang J. 2015. Rapid responses of mesophyll conductance to changes of CO_2 concentration, temperature and irradiance are affected by N supplements in rice. *Plant, Cell & Environment* 38: 2541–2550.

Xiong FS, Ruhland CT, Day TA. 1999. Photosynthetic temperature response of the Antarctic vascular plants *Colobanthus quitensis* and *Deschampsia antarctica*. *Physiologia Plantarum* 106: 276–286.

Yamori W, Hikosaka K, Way DA. 2014. Temperature response of photosynthesis in C_3, C_4, and CAM plants: temperature acclimation and temperature adaptation. *Photosynthesis Research* 119: 101–117.

Yamori W, Suzuki K, Noguchi K, Nakai M, Terashima I. 2006. Effects of Rubisco kinetics and Rubisco activation state on the temperature dependence of the photosynthetic rate in spinach leaves from contrasting growth temperatures. *Plant, Cell & Environment* 29: 1659–1670.

Zhang J, Kirkham MB. 1996. Enzymatic responses of the ascorbate–glutathione cycle to drought in sorghum and sunflower plants. *Plant Science* 113: 139–147.

Supporting Information

Additional Supporting Information may be found online in the Supporting Information section at the end of the article.

Dataset S1 Meta-data annotation list of the primary metabolite detected in this study.

Dataset S2 Fold-change (Log2) metabolite levels per temperature and species.

Fig. S1 Inferring common (conserved) and species-dependent metabolite-trait associations: two contrasting views.

Fig. S2 Metabolic responses to temperature treatments.

Fig. S3 Species-dependent metabolite-trait associations (*Colobanthus quitensis* (CQ) vs *Dianthus chinensis* (DC)).

Methods S1 Detailed explanation of biological experiments as well as statistical modeling approach.

Table S1 Gas-exchange and chlorophyll fluorescence analysis.

Table S2 Intensity values normalized by the internal standard (ribitol) and extracted sample dry weight (mg) of three secondary metabolite precursors.

Table S3 Structural leaf and physiological parameters to assess plant status between the different experiments.

Table S4 Ionomic content ratios between different organs and temperatures per each species.

Please note: Wiley Blackwell are not responsible for the content or functionality of any Supporting Information supplied by the authors. Any queries (other than missing material) should be directed to the *New Phytologist* Central Office.